



Fabrication of hydrogen-bonded metal-complex frameworks for capturing iodine



Yuanbo Xie, Fangyuan Zhong, Hongxu Chen, Danni Chen, Jiawen Wang, Junkuo Gao^{*}, Juming Yao^{**}

Institute of Fiber Based New Energy Materials, The Key Laboratory of Advanced Textile Materials and Manufacturing Technology of Ministry of Education, College of Materials and Textiles, Zhejiang Sci-Tech University, Hangzhou, 310018, China

ARTICLE INFO

Keywords:

Hydrogen-bonded metal-complex frameworks
HOF-21
Adsorption iodine
Adsorption kinetics

ABSTRACT

In this paper, novel hydrogen-bonded metal-complex frameworks MPM-1-TIFSIX and HOF-21 were selected as adsorbents to adsorb iodine. MPM-1-TIFSIX and HOF-21 were prepared by layering method and mixed stirring method, respectively. The structures of the two HOFs were characterized in detail by XRD, BET, TGA and FT-IR. The adsorption behavior and adsorption capacity of MPM-1-TIFSIX and HOF-21 for iodine were investigated in detail. The experimental data showed that the equilibrium adsorption amounts of MPM-1-TIFSIX and HOF-21 were 205.51 mg/g and 172.86 mg/g, respectively. The adsorption process of MPM-1-TIFSIX was conformed to be pseudo-second-order kinetic, while the adsorption process of HOF-21 was conformed to be pseudo-first-order kinetic. The results indicated that HOFs could be used as iodine capture and storage materials.

1. Introduction

As an important non-metallic element, iodine has a wide range of applications in chemical, pharmaceutical and life sciences [1]. In the chemical industry, the dehydrogenation of iodoalkanes is often used to produce unsaturated hydrocarbons [2]. At high temperatures, by-product hydrogen iodide continues to dehydrogenate to form iodine that is released into the atmosphere with the plant's exhaust gases. In the nuclear industry, fission of heavy nuclear elements produces thermal energy while producing some radioactive elements, including iodine [3]. Radioactive iodine elements such as I^{129} and I^{131} are easily sublimated, produce γ -rays and remain in the environment for a long time, which are very harmful to the human body and the environment [4]. At the same time, radioisotopes of iodine are used to research diseases related to the thyroid gland [5]. Once these radioactive iodine elements escape, they will cause great harm to the environment and the human body [6]. With the development of society and the advancement of technology, electronic products are becoming more and more popular, and at the same time, electronic waste is increasing [7]. According to statistics, one-tenth of the annual global gold production is used to produce electronic products [8]. At present, a mixed solution of iodine and iodide is commonly used as a leaching agent to recover gold in electronic waste

[7a,9].

Currently used iodine adsorbents include silver-plated zeolite, activated carbon, graphene aerogel and chalcogen aerogel [10]. The treatment processes include Mercurex, Iodox, electrolysis and lye elution [10c]. These adsorbents and treatment processes are capable of effectively treating iodine, but they have some disadvantages such as high cost, high equipment requirements, and intractability after-products. The emergence of new porous materials offers a variety of options for capturing iodine [11]. Metal-organic frameworks (MOFs) and covalent-organic frameworks (COFs) are novel porous materials [4b,12]. Due to their simple synthesis, high porosity, large specific surface area and adjustable structure, they have a wide range of applications in adsorption and separation [13]. Like MOFs and COFs, hydrogen-bonded organic frameworks (HOFs) are also a new type of porous materials that have been formed by hydrogen bonding in recent years [14]. HOFs are framework materials in which organic units are connected to each other by hydrogen bonding. The organic unit includes a pure organic monomer and a metal-complex. The van der Waals force, π - π stacking, halogen bond, etc. inside the HOF structure can strengthen the structure of the material [15]. Although the specific surface area of HOFs is not large compared with MOFs and COFs, which limits the application of HOFs, the specific surface area of HOFs material has been further improved with

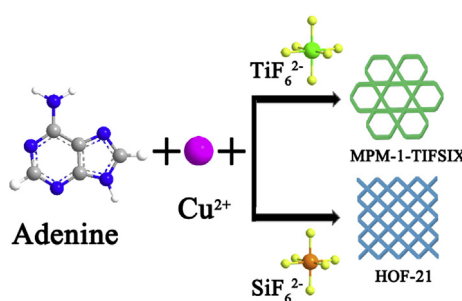
* Corresponding author.

** Corresponding author.

E-mail addresses: jkgao@zstu.edu.cn (J. Gao), yaoj@zstu.edu.cn (J. Yao).

the deepening of research. For instance, Oppel et al. successfully introduced backbones into the materials to prepare HOFs with a specific surface area of $2700 \text{ m}^2 \text{ g}^{-1}$ [16]. Compared with MOFs and COFs, HOFs also show some advantages, such as solution processability and characterization, easy purification and healing by simple recrystallization. This is mainly because hydrogen bonds are weak, flexible, directional, and reversible [17]. Therefore, HOFs have attractive research and application prospects in gas storage, carbon dioxide capture, hydrocarbon separation, molecular recognition, and optical applications [18].

Due to the inherent porosity of HOFs, it also has potential application value in adsorption. Lin et al. synthesized the elastic Hydrogen-bonded cross-linked organic framework ($\text{H}_\text{C}\text{OF}-1$) and found that $\text{H}_\text{C}\text{OF}-1$ had a good adsorption effect on iodine with a maximum adsorption capacity of 2.1 g/g [12b]. However, the structure of $\text{H}_\text{C}\text{OF}-1$ was destroyed after adsorption. Li et al. prepared π -stacked/H-bonded supramolecular organic frameworks (JLUE-SOFs) with different morphologies, and studied the adsorption properties of iodine [19]. The maximum adsorption capacity of JLUE-SOFs was 207 mg/g . Zaworotko and Chen greatly improved the stability and porosity of HOFs by introducing metal-complex inside HOFs [20]. This is advantageous for the progress of adsorption. In general, HOFs have been rarely studied in terms of iodine adsorption. So, we synthesized $[\text{Cu}_2(\text{ade})_4(\text{TiF}_6)_2]$ (MPM-1-TIFSIX, ade = adenine) according to previous reports [20a]. Different from the layering method reported in the literature, we synthesized $[\text{Cu}_2(\text{ade})_4(\text{H}_2\text{O})_2] \cdot 2\text{SiF}_6$ (HOF-21) more quickly and efficiently by stirring method [20b]. The iodine adsorption capacity of these two HOFs was further investigated (see Scheme 1). The experimental data showed that MPM-1-TIFSIX and HOF-21 had good iodine adsorption performance, and the equilibrium adsorption amounts were 205.51 mg/g and 172.86 mg/g , respectively. At the same time, the relationship between the structure and adsorption properties of these two HOFs was analyzed. At the structural level, some strategies were proposed for the synthesis of iodine adsorbents.



Scheme 1. The synthesis process of MPM-1-TIFSIX and HOF-21. Blue is a nitrogen atom; gray is a carbon atom; white is a hydrogen atom; green is a titanium atom; orange is a silicon atom; and yellow is a fluorine atom; Purple is a copper atom.

2. Results and discussion

The synthesized MPM-1-TIFSIX and HOF-21 were immersed in methanol and then dried under vacuum at 65°C . The crystal structure was tested by an X-ray diffractometer (Fig. 1). By comparison, we found that the HOF-21 prepared by the stirring method was the same as the structure prepared by the layering method. The main diffraction peaks ($2\theta = 8.3^\circ, 9.6^\circ, 10.4^\circ, 12.6^\circ, 13.3^\circ, 19.5^\circ, 21.6^\circ, 29.3^\circ$) were observed (Fig. 1a), indicating that we have successfully prepared HOF-21 using a simpler and more efficient method. Similarly, the main characteristic diffraction peaks of MPM-1-TIFSIX ($2\theta = 5.5^\circ, 7.2^\circ, 9^\circ, 9.4^\circ, 11^\circ, 13^\circ, 14.2^\circ, 15.4^\circ$) have also appeared (Fig. 1b). At the same time, we found that the structure of MPM-1-TIFSIX and HOF-21 after iodine adsorption was still maintained. The result indicated that the entry of iodine molecules did not destroy the molecular structure of both compounds.

To further understand the thermal stability of materials, thermogravimetric analysis (TG) was used to characterize the thermal stability of materials (Fig. 2). Due to the departure of the guest molecules in the pores, MPM-1-TIFSIX and HOF-21 had a small weightless platform before 100°C . Then the mass reduction of HOF-21 in the middle of $100\text{--}210^\circ\text{C}$ was caused by the departure of water molecules in the molecular structure. However, MPM-1-TIFSIX had no weight loss platform between $100\text{--}210^\circ\text{C}$.

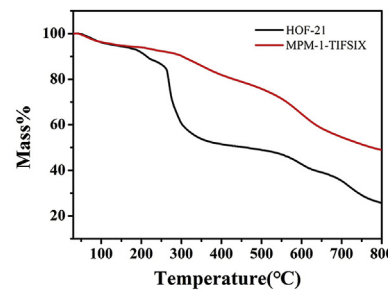


Fig. 2. The TG curves of MPM-1-TIFSIX and HOF-21.

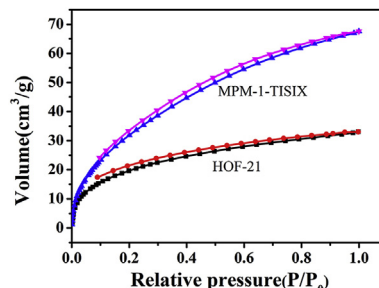


Fig. 3. CO_2 adsorption curves of MPM-1-TIFSIX and HOF-21.

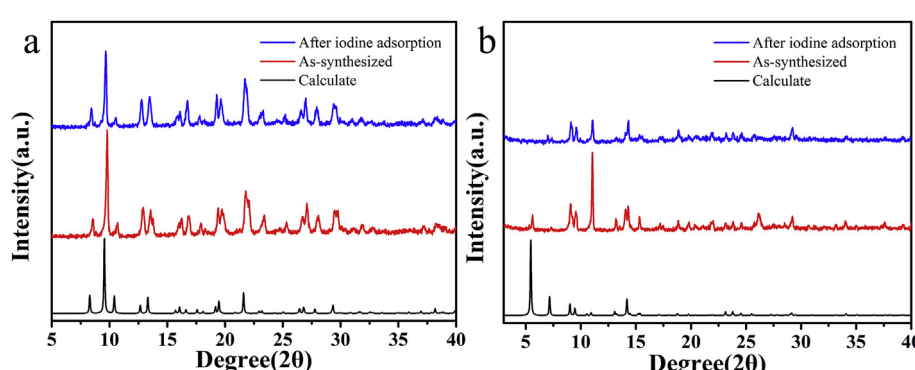


Fig. 1. a HOF-21 XRD pattern; b MPM-1-TIFSIX XRD pattern.

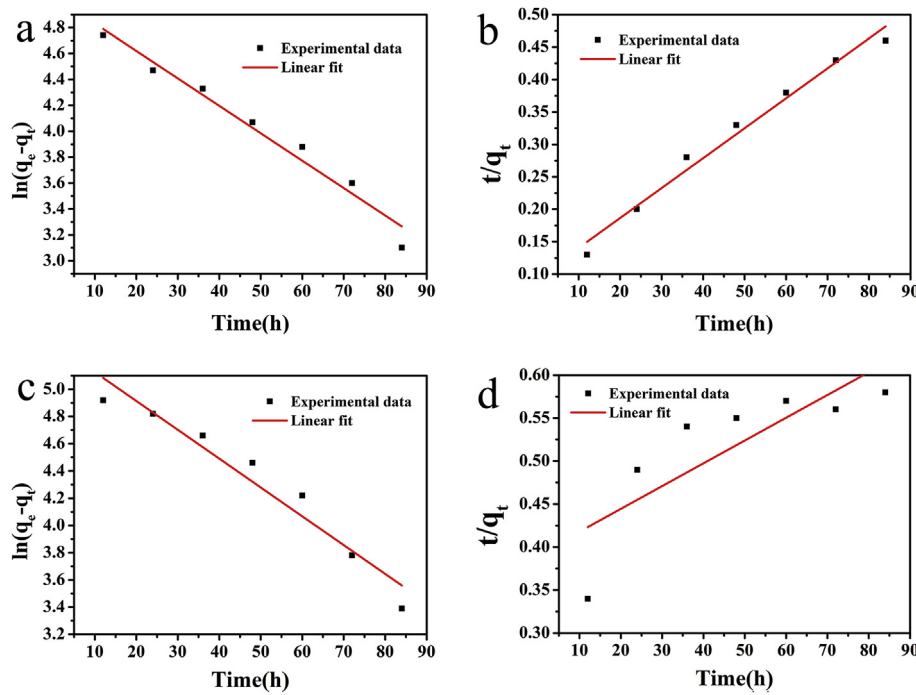


Fig. 4. Adsorption kinetic curve of MPM-1-TIFSIX and HOF-21. a and b are pseudo-first-order and pseudo-second-order curves of MPM-1-TIFSIX; c and d are pseudo-first-order and pseudo-second-order curves of HOF-21.

Table 1
Kinetics parameters of MPM-1-TIFSIX and HOF-21.

Sorbents	Pseudo-first-order kinetics		Pseudo-second-order kinetics			
	K_1 (h^{-1})	q_e (mg g^{-1})	R^2	K_2 ($g \text{ mg}^{-1}$ h^{-1})	q_e (mg g^{-1})	R^2
MPM-1-TIFSIX	0.0211	154.91	0.964	2.25×10^{-4}	216.92	0.978
HOF-21	0.0212	206.44	0.933	1.79×10^{-5}	377.36	0.603

210 °C, because there were no coordinated water molecules in the molecular structure of MPM-1-TIFSIX. Above 210 °C, the adenine ligand began to decompose. As a result, both HOFs had good thermal stability, but the difference in structure caused a difference in their thermal stability.

The porosity of the materials was confirmed by testing the CO₂ adsorption curve at 298 K (Fig. 3). Activated MPM-1-TIFSIX and HOF-21 obtained the reversible type-I CO₂ adsorption curve at 298 K. The adsorption curve indicated that both HOFs belong to the microporous material, indicating the porous structures of the both HOFs. At 298 K and 1 atm, the CO₂ adsorption capacity of MPM-1-TIFSIX was 67.6 ml/g, which was slightly less than the reported values in the literature [20a]. This indicated that the specific surface area of MPM-1-TIFSIX herein was close to that reported in the literature. The difference in specific surface area and porosity affected the amount of CO₂ adsorbed. By comparing the difference in CO₂ adsorption between HOF-21 and MPM-1-TIFSIX at 298 K and 1 atm, it was not difficult to find that the specific surface of HOF-21 was smaller than MPM-1-TIFSIX, which was consistent with the reported in the literature [20b].

The adsorption behavior was preliminarily demonstrated by dispersing 20 mg of the activated sample in 30 mL of a solution of iodine/cyclohexane (3×10^{-3} M). At the initial concentration, MPM-1-TIFSIX and HOF-21 had the highest adsorption rate. With the increase of time, the adsorption rate gradually decreases, and the adsorption equilibrium was reached in 96 h. The equilibrium adsorption amount was 205.51 mg/g and 172.86 mg/g, respectively. And as time goes on, the amount of adsorption would continue to increase. The dynamics

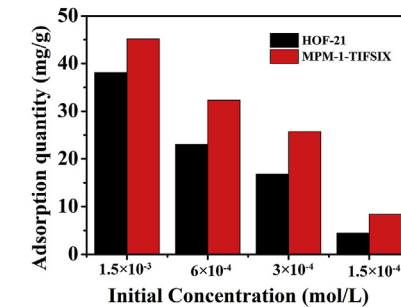


Fig. 5. The amount of adsorption of the two HOFs at different initial concentrations.

simulation curves and parameters are shown in Fig. 4 and Table 1, respectively. The R^2 of the MPM-1-TIFSIX adsorption iodine pseudo-first-order kinetic model is 0.964, and the R^2 of the pseudo-second-order kinetic model is 0.978. The R^2 of the pseudo-first-order kinetic model is slightly smaller than the R^2 of the pseudo-second-order kinetic model, which indicates that the process of adsorbing iodine by MPM-1-TIFSIX is more in line with the pseudo-second-order kinetic model. Also, the equilibrium adsorption amount (216.92 mg/g) calculated from the pseudo-second-order kinetic model is closer to the experimental data (205.51 mg/g). Interestingly, the R^2 (0.933) of the pseudo-first-order dynamic model of HOF-21 is significantly larger than that of the pseudo-second-order simulation (0.603), indicating that the process of HOF-21 adsorption of iodine conforms to the pseudo-first-order kinetic model. According to the pseudo-first-order and the pseudo-second-order kinetic model, the equilibrium adsorption amounts were calculated to be 206.44 mg/g and 377.36 mg/g, respectively. In contrast, the experimental data (172.86 mg/g) is closer to the equilibrium adsorption amount calculated by the pseudo first-order kinetic model. It can be seen that the adsorptions of iodine by MPM-1-TIFSIX and HOF-21 are two different processes, which may be related to the structure of the pores of the two HOFs. To investigate the effect of initial concentration on adsorption, 10 mg activated sample was dispersed in 15 mL of different

initial concentrations of iodine solution (1.5×10^{-3} M, 6×10^{-4} M, 3×10^{-4} M, 1.5×10^{-4} M). As can be seen in Fig. 5, the iodine adsorption of the two HOFs is small at low initial concentrations. As the initial concentration increases, the amount of adsorption also increases.

According to previous reports, paddlewheels that formed by self-assembly of central Cu^{2+} , four adenine molecules and two TiF_6^{2-} molecules constituted the network of MPM-1-TIFSIX by hydrogen bonding. This network included hourglass channels of approximately 7 Å and small triangular channels [20a]. In HOF-21, SiF_6^{2-} bridged the long band composed of dinuclear paddlewheel by hydrogen bonding and forms a two-dimensional layer. The two-dimensional layers were then further joined by SiF_6^{2-} to form a porous HOF in which there was a 3.6 Å channel. In the dinuclear paddlewheel, Cu^{2+} was coordinated with four adenine molecules and two H_2O [20b]. Different intermolecular structures lead to differences in porosity of different materials, further affecting the properties of the material. MPM-1-TIFSIX has a larger porosity than HOF-21, so MPM-1-TIFSIX has a larger adsorption amount than HOF-21. The difference in porosity and the material structure results in different adsorption amounts of the two HOFs.

The PXRD of MPM-1-TIFSIX and HOF-21 with addition of iodine is identical with the original HOFs, indicating that the structure of MPM-1-TIFSIX and HOF-21 remained the same. At the same time, FT-IR was also carried out to investigate the interaction between the two HOFs and iodine (Fig. 6). The IR spectra of the two HOFs before and after adsorption were consistent, conforming that there is no interaction between iodine and the HOFs. Based on the experimental data we measured and combining the structure of the two HOFs, we hypothesized that the adsorption mechanism of MPM-1-TIFSIX and HOF-21 was a weak electrostatic interaction between the pyrimidine ring and the iodine molecule.

3. Experimental section

3.1. Materials and general methods

$\text{Cu}(\text{NO}_3)_2 \cdot 2.5\text{H}_2\text{O}$ was provided by Wuxi Prospect Chemical Reagent Co., Ltd. (Jiangsu, China). Adenine (ade) was provided by Sun Chemical Technology (Shanghai) Co., Ltd. (Shanghai, China). $(\text{NH}_4)_2\text{SiF}_6$ and $(\text{NH}_4)_2\text{TiF}_6$ was purchased from Shanghai Maclean Biochemical Technology Co., Ltd. (Shanghai, China). Iodine was purchased by Shanghai Aladdin Biotechnology Co., Ltd. (Shanghai, China). Acetonitrile was purchased from Tianjin Komi Chemical Reagent Co., Ltd. (Tianjin, China). Methanol (MA) and Cyclohexane were supplied by Gaojing Fine Chemical Co., Ltd. (Hangzhou, China). All the chemical reagents were analytical grade and used without further purification.

The chemical structure of MPM-1-TIFSIX and HOF-21 were analyzed by FT-IR spectrometer (Nicolet 5700, Thermo Electron Corp., USA). In the range of 4000–400 cm^{-1} , it was detected by the method of KBr disk at a resolution of 4 cm^{-1} . The specific surface area was analyzed by the

Brunauer-Emmett-Teller (BET) method. The CO_2 adsorption-desorption isotherm at 298 K was measured on a Micrometrics ASAP 2010 system to analyze their pore structure. The Crystal structures of MPM-1-TIFSIX and HOF-21 were characterized by X-ray powder diffractometer (XRD, ARL X'RA, Thermo Electron Corp) with monochromatic $\text{Cu K}\alpha$ (1.54056 Å) radiation (40 kV, 40 mA) in the 2θ range of 3–40° at a scanning rate of 5°/min. The thermal stability of MPM-1-TIFSIX and HOF-21 was analyzed by thermogravimetric analyzer (TGA, Pyris Diamond I, PerkinElmer Corporation). A 3–8 mg sample was heated from 30 to 800 °C at a heating rate of 10 °C/min under a nitrogen atmosphere.

3.2. Synthesis

The preparation of MPM-1-TIFSIX and HOF-21 were based on previous reports with slight modifications [20]. The synthesis of MPM-1-TIFSIX was as follows: at room temperature, 1.5 mmol (204.9 mg) adenine was dissolved in 30 mL 1:1 acetonitrile/ H_2O , recorded as solution A; 0.76 mmol (183.6 mg) $\text{Cu}(\text{NO}_3)_2 \cdot 3\text{H}_2\text{O}$ and 0.76 mmol (150 mg) $(\text{NH}_4)_2\text{TiF}_6$ was dissolved in 30 mL water, recorded as solution B; 10 mL 1:1 acetonitrile/ H_2O was recorded as solution C. Solution C was slowly added to the upper layer of solution A, solution B was added to the upper layer of the mixed solution. The system was allowed to stand for 4 days, and the precipitate is centrifugally dried to obtain MPM-1-TIFSIX. The synthesis of HOF-21 was as follows: at room temperature, 30 mL of adenine (1.5 mmol) 1:1 acetonitrile/ H_2O was added dropwise to 30 mL of an aqueous solution of $\text{Cu}(\text{NO}_3)_2 \cdot 3\text{H}_2\text{O}$ (0.76 mmol) and $(\text{NH}_4)_2\text{SiF}_6$ (0.76 mmol), and stirred for 3 h. Then, it was centrifuged to obtain HOF-21.

3.3. Kinetics of iodine adsorption

The pseudo-first-order and the pseudo-second-order were used to analyze the adsorption behavior of the MPM-1-TIFSIX and HOF-21 [21]. The adsorption rate constant is obtained from the pseudo-first-order equation as shown below:

$$\ln(q_e - q_t) = \ln q_e - k_1 t \quad (1)$$

where q_t and q_e are the adsorption capacities (mg/g) at time t and equilibrium, and k_1 is the pseudo-first-order rate constant. From the graph of $\ln(q_e - q_t)$ versus t , the values of k_1 and q_e are determined.

The pseudo second-order dynamics model expression was as follows:

$$\frac{d_q}{dt} = k_2(q_e - q_t)^2 \quad (2)$$

The linear expression is as follows:

$$\frac{t}{q_t} = \frac{1}{k_2 q_e^2} + \frac{t}{q_e} \quad (3)$$

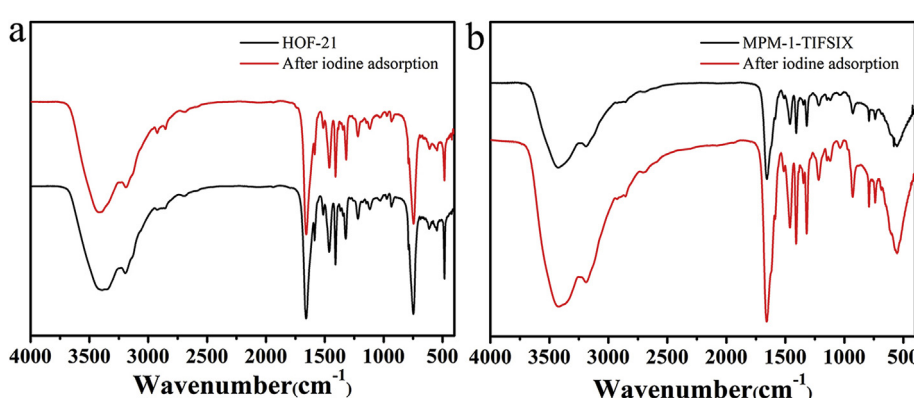


Fig. 6. FT-IR image before and after iodine adsorption of MPM-1-TIFSIX and HOF-21.

where q_t and q_e are the adsorption capacities (mg/g) at time t and equilibrium, and k_2 is the pseudo second-order rate constant and is determined from the linear plot of t/q_t versus t .

4. Conclusion

In summary, we have tried to apply HOF materials to the capture and storage of iodine, expanding the range of choices for iodine sorbents and achieving ideal results. The different construction modes of MPM-1-TIFSIX and HOF-21 result in different pore structures of the two materials, which in turn affect the adsorption capacity of the two materials. The equilibrium adsorption capacities of MPM-1-TIFSIX and HOF-21 are 205.51 mg/g and 172.86 mg/g, respectively. And as time goes on, the amount of adsorption will continue to increase. It is also recommended to design large pores and high specific surface area materials to better capture iodine molecules. Although the specific surface area of HOFs is not as large as MOFs and COFs, the amount of adsorption of HOFs is considerable. With reasonable design, the adsorption capacity of HOFs is comparable to MOFs and COFs. In pace with the deepening of research, HOFs can also occupy a place in the capture and storage of iodine like other new porous materials, and gradually replace the existing backward materials.

Acknowledgements

This work is supported by the National Natural Science Foundation of China (51672251) and Science Foundation of Zhejiang Sci-Tech University (ZSTU) under Grant No. 13012138-Y.

References

- [1] a) Z. Zhu, Y. Ma, Z. Qu, L. Fang, W. Zhang, N. Yan, Study on a new wet flue gas desulfurization method based on the Bunsen reaction of sulfur-iodine thermochemical cycle, *Fuel* 195 (2017) 33–37;
- [1] b) E. Frohlich, R. Wahl, The current role of targeted therapies to induce radioiodine uptake in thyroid cancer, *Cancer Treat Rev.* 40 (2014) 665–674;
- [1] c) P.L. Bigliardi, S.A.L. Alsagoff, H.Y. El-Kafrawi, J.K. Pyon, C.T.C. Wa, M.A. Villa, Povidone iodine in wound healing: a review of current concepts and practices, *Int. J. Surg.* 44 (2017) 260–268.
- [2] a) M.A. Gomez-Osorio, D.P. van der Sloot, L.A. Chewter, M.J. Casciato, A.D. Horton, C.M.A.M. Mesters, Capture and recovery of organic iodide species from the product stream of a process for the iodoative dehydrogenation of ethane to ethylene, *Ind. Eng. Chem. Res.* 57 (2018) 13932–13939;
- [2] b) K. Ding, A. Zhang, G.D. Stucky, Iodine catalyzed propane oxidative dehydrogenation using dibromomethane as an oxidant, *ACS Catal.* 2 (2012) 1049–1056;
- [2] c) Y.-N. Duan, Z. Zhang, C. Zhang, Recyclable hypervalent-iodine-mediated dehydrogenative cyclopropanation under metal-free conditions, *Org. Lett.* 18 (2016) 6176–6179.
- [3] D.F. Sava, T.J. Garino, T.M. Nenoff, Iodine confinement into metal–organic frameworks (MOFs): low-temperature sintering glasses to form novel glass composite material (GCM) alternative waste forms, *Ind. Eng. Chem. Res.* 51 (2011) 614–620.
- [4] a) J. Liu, R. Xiao, Y.L. Wong, X.P. Zhou, M. Zeller, A.D. Hunter, Q. Fang, L. Liao, Z. Xu, Made in water: a stable microporous Cu(I)-carboxylate framework (CityU-7) for CO₂, water, and iodine uptake, *Inorg. Chem.* 57 (2018) 4807–4811;
- [4] b) P. Wang, Q. Xu, Z. Li, W. Jiang, Q. Jiang, D. Jiang, Exceptional iodine capture in 2D covalent organic frameworks, *Adv. Mater.* (2018), e1801991;
- [4] c) D. Banerjee, X. Chen, S.S. Lobanov, A.M. Plonka, X. Chan, J.A. Daly, T. Kim, P.K. Thallapally, J.B. Parise, Iodine adsorption in metal organic frameworks in the presence of humidity, *ACS Appl. Mater. Interfaces* 10 (2018) 10622–10626.
- [5] W.P. Kluijfhout, J.D. Pasternak, F.T. Drake, T. Beninato, W.T. Shen, J.E. Gosnell, I. Suh, L.C., Q.-Y. Duh, Application of the new American Thyroid Association guidelines leads to a substantial rate of completion total thyroidectomy to enable adjuvant radioactive iodine, *Surgery* 161 (2017) 127–133.
- [6] a) K. Jie, Y. Zhou, E. Li, Z. Li, R. Zhao, F. Huang, Reversible iodine capture by nonporous pillar[6]arene crystals, *J. Am. Chem. Soc.* 139 (2017) 15320–15323;
- [6] b) Y. Liao, J. Weber, B.M. Mills, Z. Ren, C.F.J. Faul, Highly efficient and reversible iodine capture in hexaphenylbenzene-based conjugated microporous polymers, *Macromolecules* 49 (2016) 6322–6333;
- [6] c) Z.Q. Jiang, F. Wang, J. Zhang, Adsorption of iodine based on a tetrazolate framework with microporous cages and mesoporous cages, *Inorg. Chem.* 55 (2016) 13035–13038;
- [6] d) Y.Q. Hu, M.Q. Li, Y. Wang, T. Zhang, P.Q. Liao, Z. Zheng, X.M. Chen, Y.Z. Zheng, Direct observation of confined I⁻...I₂...I⁻ interactions in a metal–organic framework: iodine capture and sensing, *Chem. Eur. J.* 23 (2017) 8409–8413.
- [7] a) Z. Sun, H. Cao, Y. Xiao, J. Sietsma, W. Jin, H. Agterhuis, Y. Yang, Toward sustainability for recovery of critical metals from electronic waste: the hydrochemistry processes, *ACS Sustain. Chem. Eng.* 5 (2017) 21–40;
- [7] b) L. Zhang, Z. Xu, A review of current progress of recycling technologies for metals from waste electrical and electronic equipment, *J. Clean. Prod.* 127 (2016) 19–36;
- [7] c) M. Kaya, Recovery of metals and nonmetals from electronic waste by physical and chemical recycling processes, *Waste Manag.* 57 (2016) 64–90.
- [8] J. Cui, L. Zhang, Metallurgical recovery of metals from electronic waste: a review, *J. Hazard. Mater.* 158 (2008) 228–256.
- [9] a) A. Serpe, A. Rigoldi, C. Marras, F. Artizzu, M. Laura Mercuri, P. Deplano, Chameleon behaviour of iodine in recovering noble-metals from WEEE: towards sustainability and “zero” waste, *Green Chem.* 17 (2015) 2208–2216;
- [9] b) B. Valizadeh, T.N. Nguyen, B. Smit, K.C. Stylianou, Porous metal–organic Framework@Polymer beads for iodine capture and recovery using a gas-sparged column, *Adv. Funct. Mater.* 28 (2018) 1801596;
- [9] c) A. Akcil, C. Erust, C.S. Gahan, M. Ozgun, M. Sahin, A. Tuncuk, Precious metal recovery from waste printed circuit boards using cyanide and non-cyanide lixivians – a review, *Waste Manag.* 45 (2015) 258–271.
- [10] a) B.J. Riley, D.A. Pierce, J. Chun, J. Matyás, W.C. Lepry, T.G. Garn, J.D. Law, M.G. Kanatzidis, Polyacrylonitrile-chalcogel hybrid sorbents for radioiodine capture, *Environ. Sci. Technol.* 48 (2014) 5832–5839;
- [10] b) S.M. Scott, T. Hu, T. Yao, G. Xin, J. Lian, Graphene-based sorbents for iodine-129 capture and sequestration, *Carbon* 90 (2015) 1–8;
- [10] c) B.J. Riley, J.D. Vienna, D.M. Strachan, J.S. McCloy, J.L. Jerden, Materials and processes for the effective capture and immobilization of radioiodine: a review, *J. Nucl. Mater.* 470 (2016) 307–326;
- [10] d) B.J. Riley, J.O. Kroll, J.A. Peterson, J. Matyas, M.J. Olszta, X. Li, J.D. Vienna, Silver-loaded aluminosilicate aerogels as iodine sorbents, *ACS Appl. Mater. Interfaces* 9 (2017) 32907–32919.
- [11] a) W.-W. Xiong, J. Miao, K. Ye, Y. Wang, B. Liu, Q. Zhang, Threading chalcogenide layers with polymer chains, *Angew. Chem. Int. Ed.* 54 (2015) 546–550;
- [11] b) W.-W. Xiong, Q. Zhang, Surfactants as promising media for the preparation of crystalline inorganic materials, *Angew. Chem. Int. Ed.* 54 (2015) 11616–11623;
- [11] c) W.-W. Xiong, G. Zhang, Q. Zhang, New strategies to prepare crystalline chalcogenides, *Inorg. Chem. Front.* 1 (2014) 292–301;
- [11] d) W.-W. Xiong, E.U. Athresh, Y.T. Ng, J. Ding, T. Wu, Q. Zhang, Growing crystalline chalcogenidoarsenates in surfactants: from zero-dimensional cluster to three-dimensional framework, *J. Am. Chem. Soc.* 135 (2013) 1256–1259;
- [11] e) J. Duan, M. Higuchi, M.L. Foo, S. Horike, K.P. Rao, S. Kitagawa, A family of rare earth porous coordination polymers with different flexibility for CO₂/C₂H₄ and CO₂/C₂H₆ separation, *Inorg. Chem.* 52 (2013) 8244–8249;
- [11] f) Y. Li, M. Lu, Y. Wu, H. Xu, J. Gao, J. Yao, Trimetallic metal–organic framework derived carbon-based nanoflower electrocatalysts for efficient overall water splitting, *Adv. Mater. Interfaces* 6 (2019) 1900290;
- [11] g) Y. Dong, H. Zhang, F. Lei, M. Liang, X. Qian, P. Shen, H. Xu, Z. Chen, J. Gao, J. Yao, Benzimidazole-functionalized Zr-Uio-66 nanocrystals for luminescent sensing of Fe³⁺ in water, *J. Solid State Chem.* 245 (2017) 160–163.
- [12] a) B. Assfour, T. Assaad, A. Odeh, In silico screening of metal organic framework for iodine capture and storage, *Chem. Phys. Lett.* 610–611 (2014) 45–49;
- [12] b) Y. Lin, X. Jiang, S.T. Kim, S.B. Alahakoon, X. Hou, Z. Zhang, C.M. Thompson, R.A. Smaldone, C. Ke, An elastic hydrogen-bonded cross-linked organic framework for effective iodine capture in water, *J. Am. Chem. Soc.* 139 (2017) 7172–7175;
- [12] c) D.F. Sava, M.A. Rodriguez, K.W. Chapman, P.J. Chupas, J.A. Greathouse, P.S. Crozier, T.M. Nenoff, Capture of volatile iodine, a gaseous fission product, by zeolitic imidazolate framework-8, *J. Am. Chem. Soc.* 133 (2011) 12398–12401;
- [12] d) Y. Song, Q. Sun, B. Aguila, S. Ma, Opportunities of covalent organic frameworks for advanced applications, *Adv. Sci.* 6 (2019) 1801410;
- [12] e) J. Gao, J. Cong, Y. Wu, L. Sun, J. Yao, B. Chen, Bimetallic hofmann-type metal–organic framework nanoparticles for efficient electrocatalysis of oxygen evolution reaction, *ACS Appl. Energy Mater.* 1 (2018) 5140–5144;
- [12] f) C. Li, H. Xu, J. Gao, W. Du, L. Shangguan, X. Zhang, R.-B. Lin, H. Wu, W. Zhou, X. Liu, J. Yao, B. Chen, Tunable titanium metal–organic frameworks with infinite 1D Ti–O rods for efficient visible-light-driven photocatalytic H₂ evolution, *J. Mater. Chem. A* 7 (2019) 11928–11933.
- [13] a) W.P. Lustig, S. Mukherjee, N.D. Rudd, A.V. Desai, J. Li, S.K. Ghosh, Metal–organic frameworks: functional luminescent and photonic materials for sensing applications, *Chem. Soc. Rev.* 46 (2017) 3242–3285;
- [13] b) D. Bradshaw, J.B. Claridge, E.J. Cussen, T.J. Prior, M.J. Rosseinsky, Design, chirality, and flexibility in nanoporous molecule-based materials, *Acc. Chem. Res.* 38 (2005) 273–282;
- [13] c) B. Chen, S. Xiang, G. Qian, Metal–Organic frameworks with functional pores for recognition of small molecules, *Acc. Chem. Res.* 43 (2010) 1115–1124;
- [13] d) W. Ren, J. Gao, C. Lei, Y. Xie, Y. Cai, Q. Ni, J. Yao, Recyclable metal–organic framework/cellulose aerogels for activating peroxymonosulfate to degrade organic pollutants, *Chem. Eng. J.* 349 (2018) 766–774;
- [13] e) D.-D. Yang, Y. Song, B. Zhang, N.-N. Shen, G.-L. Xu, W.-W. Xiong, X.-Y. Huang, Exploring the surfactant–thermal synthesis of crystalline functional thioarsenates, *Cryst. Growth Des.* 18 (2018) 3255–3262;
- [13] f) P. Li, F.-F. Cheng, W.-W. Xiong, Q. Zhang, New synthetic strategies to prepare metal–organic frameworks, *Inorg. Chem. Front.* 5 (2018) 2693–2708.
- [14] S.A. Dalrymple, G.K.H. Shimizu, Crystal engineering of a permanently porous network sustained exclusively by charge-assisted hydrogen bonds, *J. Am. Chem. Soc.* 129 (2007) 12114–12116.
- [15] T. Steiner, The hydrogen bond in the solid state, *Angew. Chem. Int. Ed.* 41 (2002) 48–76.

- [16] M. Mastalerz, I.M. Oppel, Rational construction of an extrinsic porous molecular crystal with an extraordinary high specific surface area, *Angew. Chem. Int. Ed.* 51 (2012) 5252–5255.
- [17] R.B. Lin, Y. He, P. Li, H. Wang, W. Zhou, B. Chen, Multifunctional porous hydrogen-bonded organic framework materials, *Chem. Soc. Rev.* 48 (2019) 1362–1389.
- [18] J. Luo, J.-W. Wang, J.-H. Zhang, S. Lai, D.-C. Zhong, Hydrogen-bonded organic frameworks: design, structures and potential applications, *CrystEngComm* 20 (2018) 5884–5898.
- [19] Y. Li, H. Yu, F. Xu, Q. Guo, Z. Xie, Z. Sun, Solvent controlled self-assembly of π -stacked/H-bonded supramolecular organic frameworks from a C₃-symmetric monomer for iodine adsorption, *CrystEngComm* 21 (2019) 1742–1749.
- [20] a) P.S. Nugent, V.L. Rhodus, T. Pham, K. Forrest, L. Wojtas, B. Space, M.J. Zaworotko, A robust molecular porous material with high CO₂ uptake and selectivity, *J. Am. Chem. Soc.* 135 (2013) 10950–10953; b) Z. Bao, D. Xie, G. Chang, H. Wu, L. Li, W. Zhou, H. Wang, Z. Zhang, H. Xing, Q. Yang, M.J. Zaworotko, Q. Ren, B. Chen, Fine tuning and specific binding sites with a porous hydrogen-bonded metal-complex framework for gas selective separations, *J. Am. Chem. Soc.* 140 (2018) 4596–4603.
- [21] a) C. Lei, J. Gao, W. Ren, Y. Xie, S.Y.H. Abdalkarim, S. Wang, Q. Ni, J. Yao, Fabrication of metal-organic frameworks@cellulose aerogels composite materials for removal of heavy metal ions in water, *Carbohydr. Polym.* 205 (2019) 35–41; b) S. Bo, W. Ren, C. Lei, Y. Xie, Y. Cai, S. Wang, J. Gao, Q. Ni, J. Yao, Flexible and porous cellulose aerogels/zeolitic imidazolate framework (ZIF-8) hybrids for adsorption removal of Cr(IV) from water, *J. Solid State Chem.* 262 (2018) 135–141.